IJST, Transactions of Mechanical Engineering, Vol. 37, No. M2, pp 107-118
Printed in The Islamic Republic of Iran, 2013

LATTICE BOLTZMANN SIMULATION OF NATURAL CONVECTION IN PARTIALLY HEATED CAVITIES UTILIZING KEROSENE/ COBALT FERROFLUID*

GH. R. KEFAYATI**
School of Computer Science, Engineering and Mathematics, Flinders University, Adelaide, Australia
Email: gholamreza.kefayati@flinders.edu.au

Abstract– In this paper, heat dissipation effect of a ferrofluid on natural convection flow in a partially heated cavity in the presence of an external magnetic field outside of the cavity has been analyzed with lattice Boltzmann method (LBM). The cavity is filled with kerosene as the carrier fluid and nanoscale ferromagnetic of cobalt. This study has been carried out for the pertinent parameters in the following ranges: the Rayleigh number of base fluid, Ra=10^3–10^5, the volumetric fraction of nanoscale ferromagnetic between 0 and 4%, the size of the nanoscale ferromagnetic is fixed at 45nm. As the size of the heater is equal to H/3, the center of the heater is investigated at Y_p= 0.25H, 0.5H and 0.75H. Results show that the heat transfer decreases by the increase of the nanoscale ferromagnetic volume fraction for various Rayleigh numbers. The external magnetic field influences the nanoscale ferromagnetic at Ra=10^4 more than other Raleigh numbers as the least values are observed at Ra=10^3. While the heat transfer obtains the greatest value at Y_p= 0.5H for multifarious Rayleigh numbers, the greatest effect of the nanoscale ferromagnetic for Ra=10^4 and 10^5 is perceived at Y_p= 0.75H.

Keywords– Natural convection, ferrofluid, external magnetic field, cavity, LBM

1. INTRODUCTION

A magnetic colloid, also known as a ferrofluid (FF), is a colloidal suspension of single-domain magnetic particles, with typical dimensions of about 10 to100 nm, dispersed in a liquid carrier [1–3]. The liquid carrier can be polar or not polar. Since the 1960's, when these materials were initially synthesized, their technological applications have not stopped increasing.

A distinguishing feature of the research area in ferrofluids is the ample applicability of these materials. Considerable effort was made by chemists and physicists during a good part of the last century to synthesize stable magnetic fluids, motivated by the perspective of many and important technological uses. Although non-stable suspensions of magnetic particles in liquids were produced much earlier, the first synthesis of a ferrofluid was reported in the pioneering work by Papell [1], in1965. After this, an increase in scientific production took place in the area.

Of the many technological applications of magnetic fluids four main categories are singled out: a) Dynamic sealing; b) Heat dissipation; c) Damping; d) Doping of technological materials. The focus is on the heat dissipation by ferrofluid in this investigation as one way of extracting heat from equipment which heats up by functioning, and to keep it from becoming too hot, a good heat conductor which connects the equipment to some mass which has much bigger heat capacity and, perhaps, much bigger open surface to dissipate heat is used. In some cases the good heat conductor must not be a solid, because it would block

*Received by the editors November 17, 2012; Accepted May 19, 2013.
**Corresponding author

the equipment's operation (for example, if it has to vibrate). One way to achieve the desired goal is by using a ferrofluid as a heat conductor. A non magnetic liquid would flow away from the place where it is supposed to operate. A good example is a loudspeaker, whose coil heats up by functioning and the ferrofluid is kept in place by the magnetic field of the magnet which is fixed on the loudspeaker's horn. Nowadays, most of the high power loudspeakers are equipped with ferrofluid. The presence of the fluid around the coil also improves the quality of the speaker because it damps unwanted resonances which would produce a very unpleasant noise.

Khanafer et al. [4] numerically investigated buoyancy-driven heat transfer enhancement in a two-dimensional enclosure utilizing nanofluids. Their paper shows the Nusselt number for the natural convection of nanofluids is increased with the volume fraction. Jahanshahi et al [5] numerically investigated the effects due to uncertainties in effective thermal conductivity according to experimental and theoretical formulations of the SiO_2–water nanofluid on laminar natural convection heat transfer in a square enclosure. Pirmohammadi and Ghassemi [6] studied the effect of magnetic field on convection heat transfer inside a tilted square enclosure. They found that for a given inclination angle (φ), as the value of Hartmann number (Ha) increases, the convection heat transfer reduces. Furthermore, they found that at $Ra=10^4$, the value of Nusselt number depends strongly upon the inclination angle for relatively small values of Hartmann number and at $Ra=10^5$, the Nusselt number increases up to about $\varphi=45^o$ and then decreases as φ increases.

For more than one decade, LBM has been demonstrated to be a very effective numerical tool for a broad variety of complex fluid flow phenomena that are problematic for conventional methods [7-9]. LBM presents some advantages, including the physical representation of microscopic interactions, the uniform algorithm for multiphase flows, and the easiness in dealing with complex boundary. In addition, LBM-like algorithms have been developed to solve microfluidics-related processes and phenomena, such as heat transfer, electric/magnetic field, and diffusion [12]. Kefayati et al. [13] studied the effect of SiO_2/water nanofluid for heat transfer improvement in tall enclosures by LBM. They showed that the average Nusselt number increases with volume fraction for the whole range of Rayleigh numbers and aspect ratios. Furthermore, the effect of nanoparticles on heat transfer augments as the enclosure aspect ratio increases. Moreover, Kefayati et.al [14] investigated Prandtl number effect on natural convection MHD in an open cavity which has been filled respectively with Liquid Gallium, Air and Water by LBM. They exhibited heat transfer declines with the increase of Hartmann number, while this reduction is marginal for $Ra=10^3$ by comparison with other Rayleigh numbers. LBM simulation of MHD mixed convection in a lid-driven square cavity with linearly heated wall has been researched by Kefayati et al. [15]. It was shown that the augmentation of Richardson number causes heat transfer to increase, as the heat transfer decreases by the increase of Hartmann number for various Richardson numbers and the directions of the magnetic field. The highest decline of heat transfer on the linearly heated wall was found at $\theta = 0°$ for Richardson numbers of $Ri = 100$ and $Ha = 100$. On the other hand, the least effect of the magnetic field was observed at $Ri = 0.01$ from $Ha = 25$ to 100 for both directions on the linearly heated wall. Recently, Kefayati [16] conducted a research into the effect of a magnetic field on natural convection in an open enclosure which subjugated to water/copper nanofluid using LBM. It appeared that the heat transfer decreases by the increase of Hartmann number for various Rayleigh numbers and volume fractions. In addition, they mentioned the magnetic field augments the effect of nanoparticles at Rayleigh number of $Ra=10^6$ regularly.

The main aim of the present study is to identify the ability of ferrofluids to dissipate heat transfer in multifarious industries; therefore, LBM as a modern mesoscopic method is utilized to solve the problem. In fact, this study can be significant not only for the subject of the problem, but also because of the applied method (LBM) used to solve it. An attempt was made to express the best situation for heat transfer dissipation with the alterations of multifarious considered parameters. Hence, the ferrofluid on laminar natural convection heat transfer in the presence of an external magnetic field in a cavity by LBM was investigated. The effects of all parameters on flow field and temperature distribution are also considered.

2. PROBLEM STATEMENT

The geometry of the present problem is shown in Fig. 1. It consists of a two-dimensional cavity with the height of H. The temperatures of the two sidewalls of the cavity are maintained at T_H and T_C, where T_C has been considered as the reference condition. The top and the bottom horizontal walls have been considered to be adiabatic i.e., non-conducting and impermeable to mass transfer. The cavity is filled with a mixture of kerosene and nanoscale ferromagnetic of cobalt. The nanoscale ferromagnetic in the cavity is Newtonian, incompressible, and laminar. Thermophysical properties of the nanoscale ferromagnetic are assumed to be constant (Table1).The density variation in the ferrofluid is approximated by the standard Boussinesq model. The external uniform magnetic field with a constant magnitude is applied at (x=H/2 and y=1.1H).

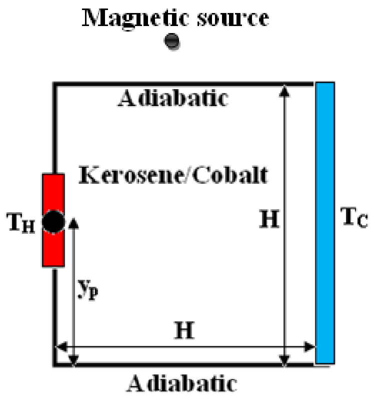

Fig. 1 Geometry of the present study

Table1. Thermophysical properties of kerosene and cobalt

Property	Kerosene	**Cobalt**
μ (kg/ms)	1.64×10^{-3}	_
c_p (j/kg k)	2090	420
ρ (kg/m^3)	780	8900
k (w/m k)	0.149	100

3. NUMERICAL METHOD

a) Lattice Boltzmann method

Standard D2Q9 for flow and temperature, and LBM method are used in this work hence, only brief discussion will be given in the following paragraphs, for completeness. The BGK approximation lattice Boltzmann equation with external forces can be written as [7],

For the flow field:

$$f_i\left(x+c_i\Delta t,t+\Delta t\right)-f_i\left(x,t\right)=-\frac{1}{\tau_v}\left[f_i\left(x,t\right)-f_i^{eq}\left(x,t\right)\right]+\Delta tF_i \tag{1}$$

For the temperature field:

$$g_i\left(x+c_i\Delta t,t+\Delta t\right)-g_i\left(x,t\right)=-\frac{1}{\tau_c}\left[g_i\left(x,t\right)-g_i^{eq}\left(x,t\right)\right] \tag{2}$$

where the discrete particle velocity vectors defined c_i , Δt denotes lattice time step which is set to unity. τ_v, τ_c are the relaxation time for the flow and temperature fields, respectively. f_i^{eq} ,g_i^{eq} are the local equilibrium distribution functions that have an appropriately prescribed functional dependence on the local hydrodynamic properties which are calculated with Eqs. (3) and (4) for flow and temperature fields respectively. Also, F_i is an external force term.

$$f_i^{eq}(x,t)=\omega_i\rho\left[1+\frac{c_i u}{c_s^2}+\frac{1}{2}\frac{(c_i u)^2}{c_s^4}-\frac{1}{2}\frac{uu}{c_s^2}\right] \tag{3}$$

$$g_i^{eq}=\omega_i T\left[1+\frac{c_i u}{c_s^2}\right] \tag{4}$$

Here u and ρ are the macroscopic velocity and density, respectively; moreover, c_s is the lattice sound speed. ω_i is weighted factor and is obtained for D2Q9 as follows:

For D2Q9

$$\omega_i=\begin{cases} 4/9 & i=0 \\ 1/9 & i=1\text{-}4 \\ 1/36 & i=5\text{-}8 \end{cases} \tag{5}$$

The discrete velocities, c_i, for the D2Q9 are defined as follows:

$$c_i=\begin{cases} 0 & i=0 \\ c\left(\cos[(i-1)\pi/2],\sin[(i-1)\pi/2]\right) & i=1\text{-}4 \\ c\sqrt{2}\left(\cos[(i-5)\pi/2+\pi/4],\sin[(i-5)\pi/2+\pi/4]\right) & i=5\text{-}8 \end{cases} \tag{6}$$

Where c=Δx/Δt, Δx and Δt are the lattice space and the lattice time step size, respectively, which are set to unity. The kinematic viscosity ν and the thermal diffusivity α are then related to the relaxation times by:

$$\nu=\left[\tau_v-\frac{1}{2}\right]c_s^2\Delta t \quad \text{and} \quad \alpha=\left[\tau_c-\frac{1}{2}\right]c_s^2\Delta t \tag{7}$$

Finally, the macroscopic quantities (ρ, u, T) can be calculated by the mentioned variables, with the following formula.

$$\text{Flow density: } \rho(x,t)=\sum_i f_i(x,t) \tag{8}$$

$$\text{Momentum: } \rho u(x,t)=\sum_i f_i(x,t)c_i \tag{9}$$

$$\text{Temperature: } \rho RT=\sum_i g_i(x,t) \tag{10}$$

Viscosity is selected to insure that Mach number is within the limit of incompressible flow (Ma<0.3) where Mach number is fixed at 0.1 in this investigation.

The viscosity is calculated by Eq.11 where Rayleigh number, Prandtl number, Mach number and the number of lattices are fixed. Subsequently, the thermal diffusivity is computed by Prandtle number.

$$\nu=\sqrt{\frac{Ma^2M^2\Pr c^2}{Ra}} \tag{11}$$

where M is number of lattices in y-direction (parallel to gravitational acceleration). Rayleigh and Prandtl numbers are defined as $Ra=\frac{\beta g_y H^3 \Pr(T_H-T_C)}{\vartheta^2}$, and $\Pr=\frac{\nu}{\alpha}$, respectively. In addition speed of lattice is constant ($c=\frac{1}{\sqrt{3}}$). Finally, the values of relaxation times for flow and temperature (Eqs.7) can be found by the obtained viscosity and thermal diffusivity.

b) Lattice Boltzmann method at the presence of the external magnetic field

The effect of the magnetic field was shown only in the force term where it is added to the buoyancy force term.

For natural convection driven flow, the force term is:

$$F_n=\rho g_y\beta\Delta T \tag{12}$$

where g_y is the gravitational vector, ρ is the density, ΔT is the temperature difference between hot and cold boundaries and β is the thermal expansion coefficient.
But for the external magnetic field, the force term is:

$$F_B=\frac{A}{r^2} \tag{13}$$

In our model, a stable magnetic field was maintained; therefore, the magnetic terms depend only on the degree of magnetization and distance from the magnetic source. A is the magnetic coefficient defined in this model. The particle size influences the degree of magnetization. It is assumed that the magnetization coefficient for a particle size of 45 nm is A=1. In addition, r is the distance of the external magnetic field and is equal to $r^2=x^2+y^2$, as it was mentioned that x=H/2 & y=1.1H.

The force is added to the collision process as:

$$F_i=3\omega_i Fc_i \tag{14}$$

where $F_i=F_B+F_n$ and the values of ω_i and c_i were shown before.

c) Lattice Boltzmann method for nanoscale ferromagnetic

The dynamical similarity depends on two dimensionless parameters: the Prandtl number *Pr* and the Rayleigh number *Ra*, where it is assumed that the mixture of the carrier fluid (kerosene) and the nanoscale ferromagnetic (cobalt) is similar to a pure fluid and then the mixture qualities are obtained and applied for the two parameters (Rayleigh and Prandtl numbers).

The thermo-physical properties of the nanofluid are assumed to be constant (Table 1) except for the density variation, which is approximated by the Boussinesq model.

The effect of density at reference temperature is given by [18]:

$$\rho_{ff}=\left(1-\varphi\right)\rho_f+\varphi\rho_{nf} \tag{15}$$

where the heat capacitance of the mixture is [17]:

$$\left(\rho c_p\right)_{ff}=\left(1-\varphi\right)\left(\rho c_p\right)_f+\varphi\left(\rho c_p\right)_{nf} \tag{16}$$

with φ being the volume fraction of the nanoscale ferromagnetic (cobalt) and subscripts *ff,nf* and *f* stand for the mixture, nanoscale ferromagnetic and the base fluid, respectively. The viscosity of the mixture containing a dilute suspension of small rigid spherical particles is given by Brinkman model as:

$$\mu_{ff} = \frac{\mu_f}{(1-\varphi)^{2.5}} \tag{17}$$

The effective thermal conductivity of the mixture can be approximated by the Maxwell-Garnetts (MG) model as [11]:

$$\frac{k_{ff}}{k_f} = \frac{k_{nf} + 2k_f + 2(k_f - k_{nf})}{k_{nf} + 2k_f - \varphi(k_f - k_{nf})} \tag{18}$$

Nusselt number *Nu* is one of the most important dimensionless parameters in describing the convective heat transport. The local Nusselt number and the average value at the hot and cold walls are calculated as

$$NU_y = -\frac{H}{\Delta T}\frac{\partial T}{\partial x} \tag{19}$$

$$NU_{avg} = \frac{1}{H}\int_0^H NU_y dy \tag{20}$$

Because of considering different parameters effect precisely, a normalized average Nusselt number is defined. The normalized average Nusselt number expresses Nusselt number at any volume fractions of the nanoscale ferromagnetic to that of pure kerosene which is written as follows:

$$NU^*_{avg}(\varphi) = \frac{NU_{avg}(\varphi)}{NU_{avg}(\varphi=0)} \tag{21}$$

Finally, the convergence criterion is defined by the following expression:

$$Error = \left| \frac{2(NU_{avg,H} - NU_{avg,c})}{NU_{avg,H} + NU_{avg,c}} \right| \le 10^{-5} \tag{22}$$

4. CODE VALIDATION AND GRID INDEPENDENCE

The problem is investigated at different Rayleigh numbers of (10^3< Ra <10^5), the external magnetic field is applied at (x=H/2, y=1.1H). LBM scheme is utilized to obtain the numerical simulations in a cavity that is filled with the mixture of kerosene/cobalt. An extensive mesh testing procedure is conducted to guarantee a grid independent solution. Five different mesh combinations are explored for the case of Ra= 10^5 at Y_p=0.5H. The present code is tested for the grid independence by calculating the average Nusselt number on the heated section. It is confirmed that the grid size (60_60) ensures a grid independent solution as portrayed by Table 2. To check the accuracy of the present results, the present code is validated with published studies in the literature on the cavity in the presence of a magnetic field [6]. The results are compared in Fig. 2 as the streamlines and the isotherms have an appropriate agreement between both compared methods. The method of solution for nanofluid with LBM is validated by the consequences of Khanafer et al. [4] and Jahanshahi et al. [5] at Fig. 3.

Table. 2 Grid independence study at Y_p=0.5H and Ra=10^5

Mesh size	NU_h
20×20	3.22
30×30	3.39
40×40	3.48
50×50	3.561
60×60	3.567
70×70	3.567

(a)

(b)

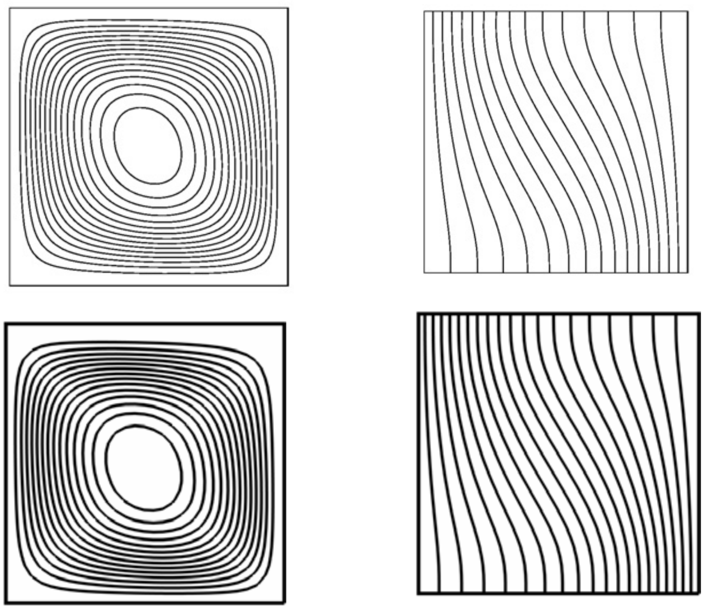

Fig. 2. Comparison of the streamlines and isotherms between (a) numerical results by Pirmohammadi and Ghassemi [6] and (b) the present results (Ra=7000, Ha=25)

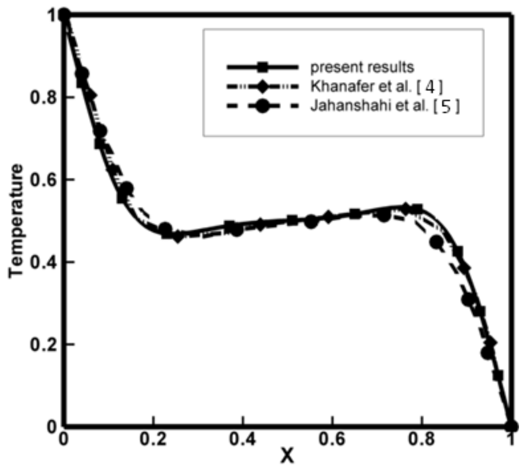

Fig. 3. Comparison of the temperature on axial midline between the present results and numerical results by Khanafer et al. [4] and Jahanshahi et al. [5] [(pr=6.2,φ=0.1,Gr=10^4)]

5. RESULTS AND DISCUSSION

a) Effect of nanoscale ferromagnetic on the isotherms

Figure 4 illustrates the effect of the external magnetic source on the isotherm of nanoscale ferromagnetic (φ=0.04) and the isotherm of the pure fluid (φ=0) simultaneously for various Rayleigh numbers and the location of the heater. It is evident that the density of the isotherm on the heater augments at Y_p=0.5H is more than the other locations of the heater; therefore, the greatest degree of heat transfer is obtained in the position (Y_p=0.5H) for various Rayleigh numbers. The isotherms behave towards the increase of nanoscale ferromagnetic volume fraction for different Rayleigh numbers and the locations of the heaters erratically; hence, the mentioned parameters are investigated respectively. At Ra=10^3, the comparison demonstrates that the curve shape of the isotherm declines as the volume fraction augments; in fact, they behave like pure conduction at φ=0.04. Moreover, it is obvious that the distance between the isotherms of φ=0 and 0.04 decreases when the heater moves upwards. Consequentially, the nanoscale ferromagnetic influences the isotherms at Y_p=0.25H significantly in comparison with other positions of the heater. The effect of the convective heat transfer is growing considerably while Rayleigh number enhances, as a result of distinct boundary layers along the active walls of the cavity. The gradient of the boundary layer decreases as a consequence of the rise of volume fraction. Therefore, the pattern results in decrease in heat transfer. At Ra=10^4, the effect of nanoscale ferromagnetic on the isotherm is more noticeable than Ra=10^3 since the influence ameliorates generally. At Ra=10^5, when the power of the convective flow enhances, the influence of the external magnetic source on the isotherms drops markedly in comparison with Ra=10^4. Meanwhile the plunge is more substantial in the core of the cavity in contrast with the near sections of the sidewalls. Furthermore, for Ra=10^4 and 10^5, the isotherms display the greatest alteration in the presence of the nanoscale ferromagnetic at Y_p=0.75H.

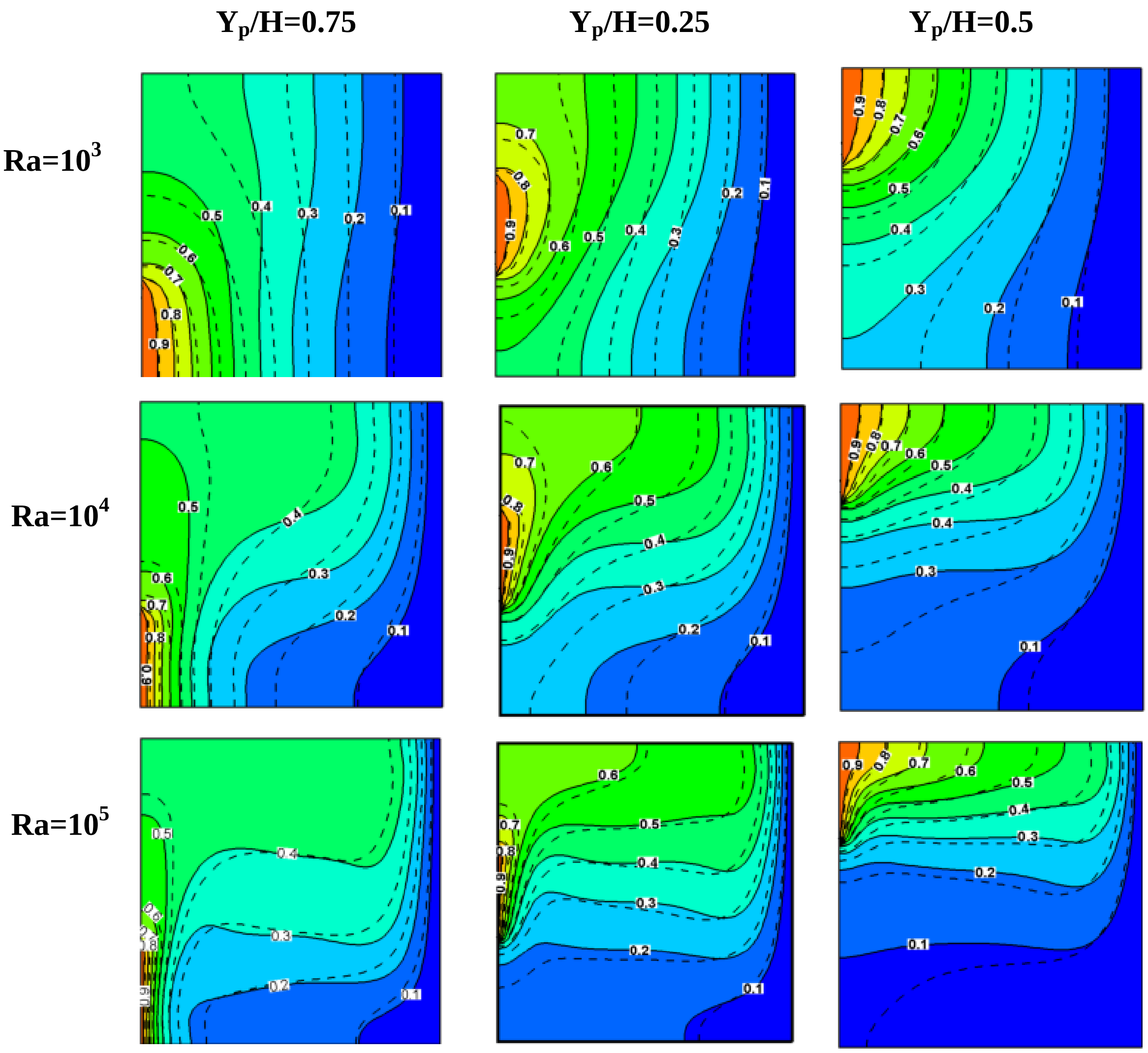

Fig. 4. Comparison of the isotherms at various Rayleigh numbers and locations of the heater (pure kerosene (-) and kerosene/cobalt with φ=0.04 (---))

b) Effect of nanoscale ferromagnetic on the streamlines

Figure 5 presents the streamlines at pure fluid (φ=0) and the presence of the nanoscale ferromagnetic (φ=0.04) for different Rayleigh numbers and the heater location of Y_p=0.5H. The effect of nanoscale ferromagnetic on the streamline is demonstrated by the form and the strength of the streamline central circulation. As the volume fraction of the nanoscale ferromagnetic increases, the maximum value of the streamline decreases. The best way to exhibit the ability of the nanoscale ferromagnetic to decrease convective flow in the cavity is a special amount of the streamline in the core of the cavity. For example, at Ra=10^3, the value is ψ=-1.9$\times 10^{-4}$as the width of the streamline is decreased by the increase in the volume fraction intensively. The trend is followed by Rayleigh numbers of Ra=10^4 and 10^5 as the streamline expansion of ψ=-1.2$\times 10^{-3}$ and -1.6$\times 10^{-3}$ respectively have been diminished by the enhancement of the volume fraction.

c) Effect of nanoscale ferromagnetic on the average Nusselt number and the dimensionless average Nusselt number

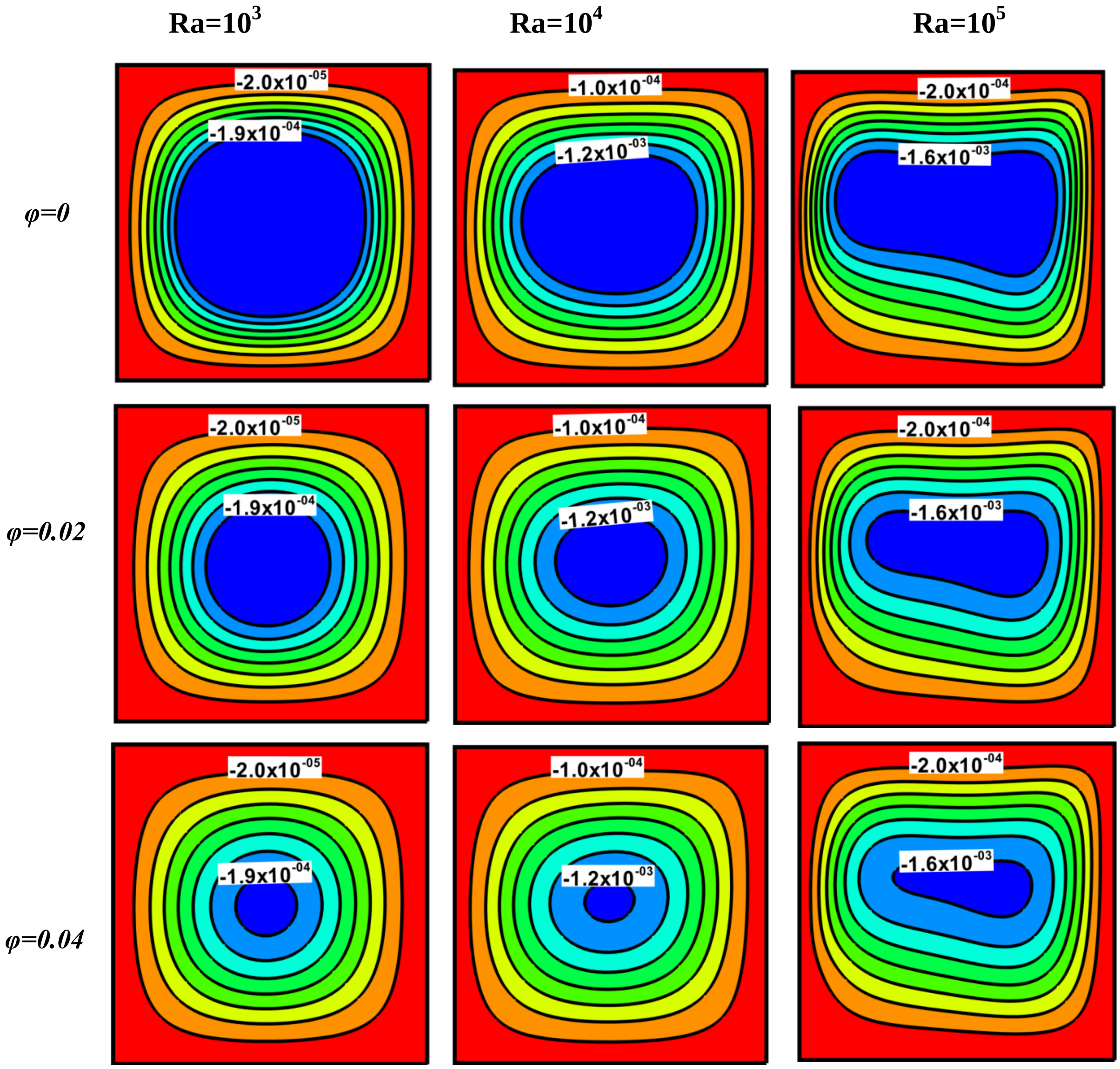

Fig. 5. Comparison of the streamlines for Y_p/H=0.5 at various Rayleigh numbers and volume fractions

Figure 6 shows comparison of the average Nusselt number and the dimensionless average Nusselt number for various Rayleigh numbers, volume fractions and the position of the heater. Generally, the average Nusselt number has obtained the greatest value at Y_p=0.5H, whereas the least average Nusselt number is revealed at Y_p=0.25H for Ra=10^4 and 10^5. The average Nusselt number demonstrates that the heat transfer drops as a result of the increase in the volume fraction of the nanoscale ferromagnetic. Indisputably, the apt parameter, to show the effect of the addition of the nanoscale ferromagnetic to the pure fluid, is the dimensionless average Nusselt number. The ratio exhibits that the growth of nanoscale ferromagnetic volume fraction provokes heat transfer to plummet for different Rayleigh numbers. It demonstrates that the nanoscale ferromagnetic influences the heat transfer extensively at Ra=10^4; albeit, the differences between values of Ra=10^5 and Ra=10^4 are marginal. However, the nanoscale ferromagnetic lack the ability to decrease heat transfer at Ra=10^3 effectively. For Ra=10^3, the fruitful shape for the improvement of ferromagnetic nanoscale impact is sensible at Y_p=0.5H where it is observed at Y_p=0.75H for Ra=10^4 and 10^5.

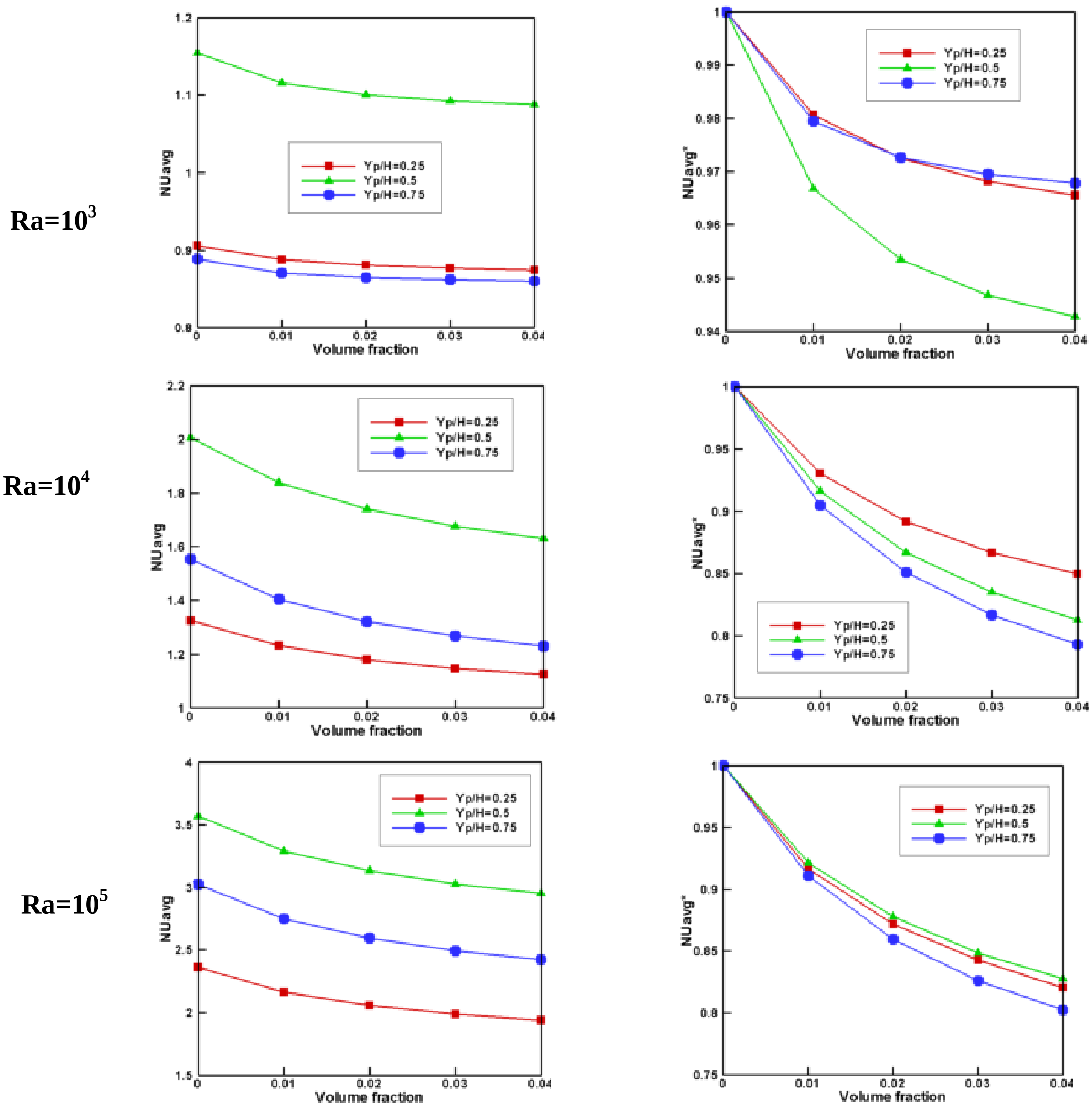

Fig. 6. Comparison of the average Nusselt number (NUavg) (a) and dimensionless average Nusselt number (NUavg*) (b) at various Rayleigh numbers, volume fractions and the locations of the heaters

6. CONCLUSION

In this paper, the effect of an external magnetic field on nanoscale ferromagnetic in a partially heated cavity has been analyzed with LBM. This study has been carried out for the pertinent parameters in the following ranges: the Rayleigh number of the carrier fluid (kerosene), Ra=10^3–10^5, the volume fraction of the nanoscale ferromagnetic (cobalt), φ=0 to 0.04, the direction of the magnetic field is fixed at X direction and different positions for the center of the heater (Y_p= 0.25H, 0.5H and 0.75H) as the size of the heater is fixed at H/3. The apt agreement is consistent with previous numerical investigations and demonstrates that LBM is an appropriate method for different applicable problems. Heat transfer declines with an increase in volume fraction of nanoscale ferromagnetic for various Rayleigh numbers albeit the trend is different for multifarious locations of the heater. The least effect of the addition of the nanoscale ferromagnetic is observed at Ra=10^3. At Ra=10^4 and 10^5 equal patterns are exhibited against the increase of the nanoscale ferromagnetic volume fraction while the heat transfer at Ra=10^4 is influenced by the volume fraction more than Ra=10^5. At Ra=10^4 and 10^5, the greatest heat dissipation effect of the ferrofluid is found for Y_p=0.75H.

NOMENCLATURE

B	magnetic field
c	lattice speed
c_i	discrete particle speeds
c_p	specific heat at constant pressure
F	external forces
f	density distribution functions
f^{eq}	equilibrium density distribution functions
g	internal energy distribution functions
g^{eq}	equilibrium internal energy distribution functions
g_y	gravity
M	Lattice number
Ma	Mach number
Nu	Nusselt number
Pr	Prandtl number
R	constant of the gases
Ra	Rayleigh number $\left(Ra=\dfrac{\beta g_y H^3 (T_H - T_C)}{\nu\alpha}\right)$
T	temperature
x,y	cartesian coordinates
u	velocity magnitude

Greek letters

σ	surface tension
ω_i	weighted factor indirection i
β	thermal expansion coefficient
τ_c	relaxation time for temperature
τ_v	relaxation time for flow
ν	kinematic viscosity
Δx	Lattice spacing
Δt	time increment
α	thermal diffusivity
φ	volume fraction
μ	dynamic viscosity
ψ	stream function value
θ	inclination angle

Subscripts

avg	average
C	cold
H	hot
f	fluid
nf	nanoscale ferromagnetic
ff	ferrofluid

REFERENCES

1. Papell, S. S. (1965). Low viscosity magnetic fluid obtained by the colloidal suspension of magnetic particles. *U. S. Patent 3*, Vol. 215, p. 572.
2. Rosensweig, R. E. (1997). *Ferrohydrodynamics*. Cambridge Univ. Press, Cambridge, London, 1985; republished by Dover. Publ. Inc., New York.
3. Cheng, W. T. & Cheng, H. W. (2009). Synthesis and characterization of cobalt nanoparticles through microwave polyol process. *AIChE Journal*, Vol. 55, pp. 1383–1389.

4. Khanafer, K., Vafai, K. & Lightstone, M. (2003). Buoyancy-driven heat transfer enhancement in a two-dimensional enclosure utilizing nanofluids. *International Journal of Heat and Mass Transfer*, Vol. 46, pp. 3639–3653.
5. Jahanshahi, M., Hosseinizadeh, S. F., Alipanah, M., Dehghani, A. & Vakilinejad, G. R. (2010). Numerical simulation of free convection based on experimental measured conductivity in a square cavity using Water/SiO_2 nanofluid. *International Communications in Heat and Mass Transfer*, Vol. 37, pp. 687–694.
6. Pirmohammadi, M. & Ghassemi, M. (2009). Effect of magnetic field on convection heat transfer inside a tilted square enclosure. *International Communications in Heat and Mass Transfer*, Vol. 36, pp. 776–780.
7. Mohamad, A. A. & Kuzmin, A. (2010). A critical evaluation of force term in lattice Boltzmann method, natural convection problem. *International Journal of Heat and Mass Transfer*, Vol. 53 pp. 990–996.
8. Sajjadi, H., Gorji, M., Hosseinzadeh, S. F., Kefayati, G. R. & Ganji, D. D. (2011). Numerical Analysis of turbulent natural convection in square cavity using large-eddy simulation in Lattice Boltzmann method. *Iranian Journal of Science and Technology, Transactions of Mechanical Engineering*, Vol. 35, pp. 133-142.
9. Sajjadi, H., Gorji, M., Kefayati, G. H. R. & Ganji, D. D. (2012). Lattice Boltzmann simulation of turbulent natural convection in tall enclosures using Cu/Water nanofluid. *Numerical Heat Transfer, Part A*, Vol. 62, pp. 512–530.
10. Kefayati, GH. R. (2013). Lattice Boltzmann simulation of natural convection in nanofluid-filled 2D long enclosures at presence of magnetic field. *Theoretical and Computational Fluid Dynamics*, Vol. 27, pp. 865-883.
11. Kefayati, GH. R. (2013). Lattice Boltzmann simulation of MHD natural convection in a nanofluid-filled cavity with sinusoidal temperature distribution. *Powder Technology*. Vol. 243, pp. 171-183.
12. Zhang, Z. (2011). Lattice Boltzmann method for microfluidics: models and applications. *Microfluidics and Nanofluidics*, Vol. 10, pp. 1-28.
13. Kefayati, GH. R., Hosseinizadeh, S. F., Gorji, M. & Sajjadi, H. (2011). Lattice Boltzmann simulation of natural convection in tall enclosures using water/ SiO_2 nanofluid. *International Communications in Heat and Mass Transfer*, Vol. 38, pp. 798-805.
14. Kefayati, GH. R., Gorji, M., Ganji, D. D. & Sajjadi, H. (2013). Investigation of Prandtl number effect on natural convection MHD in an open cavity by Lattice Boltzmann Method. *Engineering Computations*, Vol. 30, pp. 97-116.
15. Kefayati, GH. R., Gorji, M., Sajjadi, H. & Ganji, D. D. (2012). Lattice Boltzmann simulation of MHD mixed convection in a lid-driven square cavity with linearly heated wall. *Scientia Iranica*, Vol. 19, No. 4, pp. 1053−1065.
16. Kefayati, GH. R. (2013). Effect of a magnetic field on natural convection in an open cavity subjugated to Water/Alumina nanofluid using Lattice Boltzmann Method. *International Communications in Heat and Mass Transfer*, Vol. 40, pp. 67–77.
17. Chang, C. M., Cheng, W. T., Liu, W. J., Cheng, H. W., Huang, C. E. & Du, S. W. (2010). Thermal flow of fluid with magnetic particles in the presence of magnetic field. *International Communications in Heat and Mass Transfer*, Vol. 37, pp. 801–808.
18. Maxwell, J. (1904). *A treatise on electricity and magneticism*. second ed., Oxford University Press, Cambridge, UK.